Modeling of Hydraulic Jump Generated Partially on Sloping Apron

Shaker Abdulatif Jalil
Water Resources Engineering Department, College of Engineering, University of Duhok
shaker.abdulatif@uod.ac

Abstract

Modeling aims to characterize system behavior and achieve simulation close as possible of the reality. The rapid energy exchange in supercritical flow to generate quiet or subcritical flow in hydraulic jump phenomenon is important in design of hydraulic structures. Experimental and numerical modeling is done on type B hydraulic jump which starts first on sloping bed and its end on horizontal bed. Four different apron slopes are used, for each one of these slopes the jump is generated on different locations by controlling the tail water depth. Modelling validation is based on 120 experimental runs which they show that there is reliability. The air volume fraction which creates in through hydraulic jump varied between 0.18 and 0.28. While the energy exchanges process take place within 6.6, 6.1, 5.8, 5.5 of the average relative jump height for apron slopes of 0.18, 0.14, 0.10, 0.07 respectively. Within the limitations of this study, mathematical prediction model for relative hydraulic jump height is suggested.The model having an acceptable coefficient of determination.

Keywords: Hydraulic Jump type B; jump aeratio; Relative jump height;Relative Jump Length; Sequence Depth;

االخـــــلاصه

نمذجة القفزة الهيدروليكية التي تتولد جزئيا على سطح منحدر

تهدف النمذجة الى وصف سلوك النظم وتحقيق محاكاة بموثوقية قريبة من الواقع قدر الامكان. أن التبادل السريع بين انواع الطاقة في القفزة الهيدروليكية (المائية) والتى يتحول فيها الجريان من جريان فوق الحرج الى جريان هادئ ، حيث بعتبر هذا التبادل في الطاقة مهم في تصاميم المنشأت الهيدروليكية. تم إجراء تجارب مختبرية على القفزة الهيدروليكة من النوع B التي تبدأ على السطح منحدر وتنتهي في الجزء المستوي من القناة. أستخدم في التجربة اربعة منحدرات مختلفة ، حيث تم التحكم في موقع حدوث القفزة الهيدروليكية على السطح المنحدر بواسطة تنظيم عمق الماء في نهاية القناة. أظهرت المقارنة بين البيانات المختبرية ل 120 تجربة مع مرادفاتها من المحاكاة بأن هناك موثوقية مقبولة. كما ان نسبة الهواء الذى يخترق القفزة يتراوح بين 0.18 الى 0.28 ، في حين أن عملية تبادل الطاقة تجري في 6.6 و 6.1 و 5.8 و 5.5 من متوسط ارتفاع القفزة النسبية لمنحدرات 0.18، 0.14، 0.10، 0.07 على التوالي. كما تم اقتراح نموذج رياضي للتنبؤ بالارتفاع النسبي للقفزة الهيدروليكية.

الكلمات المفتاحية: القفزة الهيدروليكية النوع B ، التهوية في القفزة ، الارتفاع النسبي للقفزة ، الطول النسبي للقفزة ، الأعماق المترادفة للقفزة.

Introduction

The outlet flow from many hydraulic structures may be supercritical. This type of flow need to be reduced its kinetic energy. As early as had done by Leonardo da Vinci 1452 – 1519, who had observed flow of floating body's in hydraulic jump. Da Vinci made notes for description the movement of water by drawing and explenation including eddies in water jumps, (Boucher *and* Nakayama, 1999). Later theoretical foundations for this phenomena were derived by employing momentum and continuity concept, this first was done by Belanger on 1828 (Chanson, 2008). The properties of hydraulic jump on smooth bed conditions is widely studied by (Peterka, 1984), other studies concentrated on roughened beds effect on hydraulic characteristics such as (Carollo *et.al.*,2007) and (Imran *and* Akib, 2013). Many investigations carried out to study of the effect of obstacles, baffles, steps and weirs on hydraulic jump properties such as (Negm *et.al.*, 2003) and (Kim *et.al.*, 2015). As hydraulic jump can be occur on different geometric cross-sections and on different roughness beds and slopes. Researchers studied all these possibilities experimentally and by modeling. The models of hydraulic jump is created by numerical simulation, whereas simulations based on solving partial differential equations (PDE) of

continuity and momentum. A wide explanation has been stated in doctoral thesis for modeling hydraulic jumps includes also process air and water mixing (Witt, 2014). Usually the solutions of PDE based on turbulent models. The turbulent models depend on the scheme of solving Reynolds stresses (Versteeg *and* Malalasekera, 2007). An experimental study of measuring the velocity field in submerged hydraulic jump and comparison with five different turbulence models leads to a better predictions of horizontal velocity by implementing Reynolds stress model (Gumus *et. al* , 2016). The renormalization turbulence group (RNG) model was utilized to validate undular jump, the results are compared with experimental data and good agreement found (Rostami *et.al.*,2013). The same turbulence model (RNG) was utilized and compared with experimental data to validate that rectangular strip on channel bed have a positive effect on the characteristics of a hydraulic jump (Velioglu, *et. al.* , 2015). The standard k-ε and RNG models were used to study performance of hydraulic jump in stilling basin. RNG model shows closer to predict velocity, pressure and Froude numbers (Babaali *et.al*.,2014). Numerical analysis of hydraluic jump over an obstacle using turbulent Prandtl model of k - ε and comparison with Chanson experimental results lead to that increasing Reynolds number for incoming flow to hydraulic jump, causing more gas influence on the liquid phases and the pressure gradient affect the reverse flow (Mouangue *et. al*., 2013 ;Saeed-Reza *et.al*., 2007) studied the characterics of turbulent flow in hydraulic jump by making comparison between chanson experimental measures and that of prediction from the commercial FLOW-3D® finite volume flow solver. Saeed investigation employed two turbulent models, the k-ε and RNG, to study the transition of horizontal velocity in hydraulic jump. The study shows that the predicted x direction velocity component is very similar to Chansons experimental data using RNG turbulent model in the aerated zone. Abbaspour *et.al.*, 2009 studied the velocity profile and the character of hydraulic jump which was generated of corrugated bed. Experimental measures and 2D numerical of two different turbulent models (k - ε and RNG) with the 2-phase flow theory were compared. The study shows that there is a linear relationship between the dimensionless length scale and dimensionless longitudinal distance for the velocity profile. The model RNG shows closer to experimental data and to that data obtained by Ead and Rajaratnam. Jump on sloping bed with positive and negative step was studied by Husain *et.al.*,1994, sequent depth ratio and length characteristics were compared with the earlier studies carried by USBR and Wielogorski, the study showed that stability and compactness of hydraulic jump are better on negative step. A wide empirical equations proposed and documented in different studies has been verified by Schulz *et.al*., 2015, the verification based on comparsion with simulation results of traditional k - ε turbulence model using CFX (Ansys) software. Schulz *et. al*. study includes different hydraulic jump characteristics such as roller length, sequent depth and free surface profile. The results of this study leads to conclude that the predictive equations are good for pre-design of hydraulic jump profile and the numerical simulation can view hydraulic characteristics of the prototype scale avoiding building actual physical models. An experimental study carried by (Carollo *et. al.*, 2013) on hydraulic B-jump which has a toe on the slope bed and its roller ends on horizontal part of the channel. The channel bed was roughed by gravel particles; study has concluded that roughness on the bed reduces the sequent depth ratio of a hydraulic jump when it compared with the smooth bed.

The present study is carried on to measure main jump characteristics and validation of numerical model. The type of hydraulic jump is that one which started first on sloping-apron and its end on horizontal bed. The study is valid for range of Froude and Reynolds numbers $2.5 < Fr_1 < 5.4$, $6.6 \times 10^3 < Re < 1.8 \times 10^4$, respectivly.

Theoretical Background

A good basic background on the hydraulic jump theory can be found in chapter 4 written by Rajaratnam and edited (Chow, 1967). Rajaratnam explains and study many details on hydraulic jump characteristic such as length of jump, pressure field, mean velocity, shear stress, turbulence, dissipation, air entrainment, bed velocity and even jumps on sloping channels. Theoretical bases also can be found in (Subramanya, 2009) book. Physical properties of hydraulic jump are affected by incoming flow and geometrical properties of channel (Chow, 1959;Henderson,1966).Many investigations carried on the effect of channel geometry and bed roughness on hydraulic jump characteristics, (Hughes *and* Flack, 1984) proposed approximation for a theoretical hydraulic jump equation, this approximation is close to observed characteristics. Hydraulic jump transition region length has been studied by (Sitong *and* Rajaratnam, 1996), the study showed that velocity profile in region takes semilogarithmic shape, and bed shear stress decreases to reach a constant value. Useful theoretical and experimental studies can be followed such as (Afzal *and* Bushra, 2002), in which the structure of hydraulic is compared with earlier experimental studies.

Modeling is a solving tool aims to characterize systems behavior and perform simulations close to reality. Fluid flow simulation technique is an art of mathematical operations carried on to solve the partial derivative forms of conservative equations. The mathematical representation of mass and momentum statement are presented in differential forms in equation (1) and (2) respectively. These equations are well known as Navier-Stokes since early 1800s.

$$\frac{\partial}{\partial x_i}(\rho\, U_i) = 0 \quad \dots\dots\dots\dots\dots\dots\dots\dots\dots\dots\dots\dots\dots\dots\dots\dots \quad (1)$$

$$\frac{\partial(\rho U_i)}{\partial t} + \frac{\partial}{\partial x_j}\left(\rho U_i U_j - \tau_{i\,j}\right) + \frac{\partial P}{\partial x_i} - S_M = 0 \quad \dots\dots\dots (2)$$

Where ρ is fluid density, U is the velocity, τ is molecular stress tensor, P is the pressure and S_M is source term. In many engineering practices the ratio of inertia forces to viscous forces increases so a turbulent flow generated. This flow has chaotic and random fluctuations state of velocity components with time. Reynolds decomposition method with statistics and fundamental of micro-scale theory of Kolmogorov (see Versteeg *and* Malalasekera, 2007) made a simplification to understand and solve such complicated flow structure. The velocity ($u^{/}$) and pressure ($P^{/}$) are the main fluctuating flow parameters of turbulent flow which can be presented by time average rule.

The molecular stress can be expressed as $\tau_{i\,j} = \left[\mu\left(\frac{\partial U_i}{\partial x_j} + \frac{\partial U_j}{\partial x_i}\right)\right]$ for Newtonian incompressible flow where μ is laminar viscosity and by substituting the time average rule, the time average form mass and momentum equations became as:

$$\frac{\partial}{\partial x_i}(\rho\, \bar{U}_i) = 0 \quad \dots\dots\dots\dots\dots\dots\dots\dots\dots\dots\dots\dots\dots\dots\dots\dots \quad (3)$$

$$\frac{\partial}{\partial x_j}\left(\rho\bar{U}_i\bar{U}_j - \bar{\tau}_{i\,j}\right) + \frac{\partial \bar{P}}{\partial x_i} - \bar{S}_M = \frac{\partial}{\partial x_j}\left(-\rho\bar{u_i}\bar{u_j}\right) \quad \dots\dots\dots (4)$$

The term $\frac{\partial}{\partial x_j}\left(-\rho\bar{u_i}\bar{u_j}\right)$ is Reynolds stress which represents six shearing deformations. Reynolds stresses is solved by the concept of Boussinesq eddy - viscosity. This hypothesis is based on the assumption between the viscous stresses and strain in laminar Newtonian flow as:

$$\left(-\rho\bar{u_i}\bar{u_j}\right) = \mu_t\left(\frac{\partial \bar{U}_i}{\partial x_j} + \frac{\partial \bar{U}_j}{\partial x_i}\right) - \frac{2}{3}\left(\rho k \delta_{i\,j}\right) \quad \dots\dots\dots\dots\dots (5)$$

Where, k is the turbulence kinetic energy, μ_t is the turbulent or eddy-viscosity, δ

$_{i\,j}$ is Kronecker delta and $\left(\frac{\partial \bar{U}_i}{\partial x_j}+\frac{\partial \bar{U}_j}{\partial x_i}\right)$ is the mean rate of strain. The eddy-viscosity is a hypothetical property which relates to turbulence state which may vary from point to another (Versteeg *and* Malalasekera, 2007). Depending on these hypotheses and time-averaged the momentum equation became:

$$\frac{\partial}{\partial x_j}\left(\rho\bar{U}_i\bar{U}_j-\bar{\tau}_{i\,j}\right)+\frac{\partial \bar{P}}{\partial x_i}-\bar{S}_M=\frac{\partial}{\partial x_j}\left(\mu_{eff}\frac{\partial \bar{U}_i}{\partial x_j}\right) \ldots\ldots(6)$$

Where μ_{eff} is effective viscosity and is equal to $\mu_{eff}=\mu+\mu_t$ and $\mu_{eff}\frac{\partial \bar{U}_i}{\partial x_j}$ is the total mean shear stress. The models which take above concept are known as eddy-viscosity closure models. The numerical solution will depend on number of extra terms included in algorithm. The number of terms inter the model will affect stability and economy of the modle for flow prediction, (Davidson, 2017). The modification of (Yakhot *and* Orszag, 1986) on the standard *k-ε* model by application of statistical technique (Renormalization Group) view the effect of small scale in Navier-Stokes equations with the improvement of the rapidly strain flow. Furthermore this model (RNG *k-ε*) represents better performance as it contains additional tem in ε equation for interaction between turbulence dissipation and mean shear (Yakhot *et. al.*, 1991). In additional this model takes in to account the swirl effect. The transport equations of the turbulence kinetic energy, *k*, and its rate of dissipation, ε, is presented by (Yakhot *and* Smith, 1992) and (Versteeg *and* Malalasekera, 2007) as follows:

$$\frac{\partial(\rho k)}{\partial t}+div(\rho kU)=div\left[\sigma_k\mu_{eff}\,grad\,k\right]+2\mu_t S_{ij}S_{ij}-\rho\varepsilon \ldots\ldots(7a)$$

$$\frac{\partial(\rho\varepsilon)}{\partial t}+div(\rho\varepsilon U)=div\left[\sigma_k\mu_{eff}\,grad\,\varepsilon\right]+C_{1\varepsilon}^{*}\frac{\varepsilon}{k}2\mu_t S_{ij}S_{ij}-C_{2k}^{*}\rho\frac{\varepsilon^2}{k} \ldots\ldots(7b)$$

Where: $\mu_t=\rho C_\mu\frac{k^2}{\varepsilon}$, $C_{1\,\varepsilon}^{*}=C_{1\varepsilon}-\frac{\eta\left(1-\frac{\eta}{\eta_o}\right)}{1+\beta\eta^3}$, $\eta=\left(2S_{i\,j}S_{j\,i}\right)^{1/2}\frac{k}{\varepsilon}$

While the adjustable constants are:

$C_{1\varepsilon}=1.42;\ \ C_{2\,\varepsilon}=1.68;\ \ C_\mu=0.0845;\ \ \sigma_k=\sigma_\varepsilon=1.39;\ \ \beta=0.012\ and\ \eta_o=4.377$

The computational fluid dynamic modelling software FLOW-3D has developed and commercialized by Flow-Science Inc. including five turbulence models. one of these models is RNG turbulence models which is recommended when chaos flow and unstable motion of fluid flow occur due to the generation of eddies of various sizes in additional air entrainment model can be activated. (Flow-3D, 2012), also this model shows a better transition of velocity in hydraulic jump than k-ε turbulent model (Saeed-Reza *et al.*, 2007). The flow pattern upstream gate and downstream including hydraulic jump is simulated using RNG *k-ε* model since part of the flow domain is turbulent, as presented in figure (1). Figure (1) is a definition sketch shows the parameters measured experimentally and output findings from modeling.

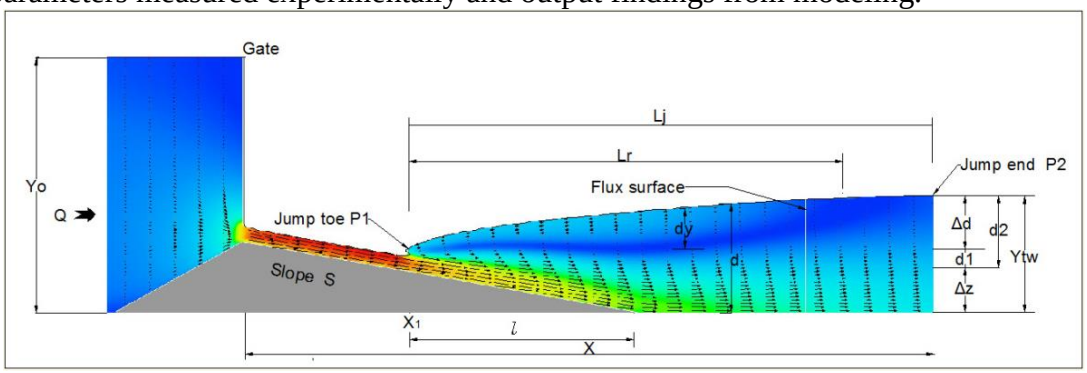

Figure (1): Flow-3D Snap with definition sketch

Experimental Work

Experimental part of the study was carried out in a horizontal rectangular cross section flume of working length 2.4 m, 0.25m height and 0.075m width. The sloping aprons were made of Mahogany wood having the slope (S) of 0.18, 0.14, 0.12 and 0.08. The Sloping aprons were fixed under the sluice gate as presented in Figure (2). The downstream water depth (Y_w) was controlled by floppy gate at the end of the channel. The water depth was measured at the center line by means of point gauge with venier. The depth in front of the gate (Ho) was also measured as boundary condition for modeling, more over the stating position of jump (P_1) on slope apron was measured. The end of jump was measured at a location (P_2) where nearly smooth horizontal flow. The location of P_2 was believed to be the end of jump.

Figure (2): Plate of sloping apron and jump

The laboratary measurements show that the jump toe is in fluctuated frequency, this frequency makes the average position of jump starting point is varied around the mean location of its occurrence. This fluctuation has found by Zhang *et.al.*, 2013. There were some visual difficulties in locating the end of hydraulic jump due to waves, oscillating fluctuations and turbulence, so the measurments of jump length (Lj) are done according to that distance which started from the toe to a position of surface stagnation according to experiments of (Karbasi, 2016). Also the end of recirculation region or surface rollers (Lr) is a challenge for locating its end. This region depends on percentage of air bubble entrainment and on Froude number of incoming flow, (Murzyn *and* Chanson, 2008).

Numerical Modeling

The geometry of the model was generated by FLOW-3D® tools. Sloping solids parts of the domain geometry were prepared by AutoCAD software as STL files which were imported to the main domain of flow. The set-up of simulations were the same for all runs such as the selection of free surface or sharp interface, air entrainment, gravitational acceleration in the vertical direction, surface tension, viscous flow, Renormalized group turbulence model (RNG k- ε) and Nonslip wall shear boundary. A structured finite volume for the computational domain was used. As the mish size has a direct effect the accuracy and time consuming of computation, the first models started with a size of 2 cm then reduced to 1 cm and later to 5 mm .The desire value of discretization 5 mm shows an acceptable shape of hydraulic jump. All models have the same boundary condition; the flow domain was fixed as symmetry at the top while the bottom and the two sides as a wall, the upstream and downstream conditions were substituted in pressure, its values were corresponding to those experimental measurements. The upstream condition is the depth of water in front of gate, while the tail water depth at the end of channel is the downstream condition. Three flux Baffles were placed along the channel length to predict the flow discharge. FLOW-3D® package includes two pressure velocity coupling solvers, the solvers based on semi-implicite numerical techniques, the first algorithm is successive over relaxation (SOR) and the second is generalized minimum residual

(GMRES) (Flow-3D, 2012). As documented in FLOW-3D® manual, the two solver algorithms show fairly similar results, the first solver is very similar to the Jacobi method which has been run slightly faster than the second. The (GMRES) algorithm solves the fully coupled system of equations which consumes time.

Results And Discussion

Verification of numerical model has been done by comparison with the experimental data. Five different laboratory measurements were used for validation of model. The measurements were the flow discharge (Q), dimensionless flow discharge under gate $\left(Fr_g = \frac{Q}{B.W\sqrt{gW}}\right)$, where B is gate width and W is gate opening. The other three measurements are depth of water before jump (d_1), location of hydraulic jump toe from the gate (P_1) and the length of the jump (Lj). Two data groups are prepared first from laboratory measurements and the second from simulations output. The data of 120 tests for each group have five measurements for each one; they are tested for homogeneity of two samples. The T-test was used to indicate whether there is difference between two independent groups. The results of test include mean, standard deviation and standard error, test results are listed in table (1 and 2) for confidence 95%. Results in table (2) show that the value of zero is located in between the lower and upper values, that means values of two samples are in homogeneity.

Table(1) Descriptive statistics for five different measures with units

Group Statistics					
Measures and units	**Group**	**N**	**Mean**	**Std. Deviation**	**Std. Error Mean**
Discharge (Q) (l/s)	1	120	.8532446	.2267901	.0207030
	2	120	.8486859	.2274116	.0207597
Frg	1	120	3.1939200	.8693151	.0793572
	2	120	3.0628654	.8284760	.0756292
d1 (mm)	1	120	10.2245560	1.1709627	.1068938
	2	120	10.1400000	.7996278	.0729957
Jump occurrence Location (P1) (cm)	1	120	16.0041667	5.7629707	.5260848
	2	120	15.8447917	5.8900553	.5376860
Jump Length (Lj) (cm)	1	120	35.6383333	9.2139753	.8411170
	2	120	35.9000000	7.1228454	.6502238

Table(2) Independent sample T- test

Independent Samples Test										
		Levene's Test for Equality of Variances		t-test for Equality of Means						
									Difference	
		F	Sig.	t	df	Sig. (2-tailed)	Mean Difference	Std. Error Difference	Lower	Upper
Discharge (Q)	Equal variances assumed	.001	.980	.155	238	.877	.00455868	.02931862	-.05319847	.06231582
	Equal variances not assumed			.155	237.998	.877	.00455868	.02931862	-.05319847	.06231582
Frg	Equal variances assumed	.411	.522	1.195	238	.233	.13105467	.10962365	-.08490189	.34701123
	Equal variances not assumed			1.195	237.451	.233	.13105467	.10962365	-.08490445	.34701378
d1	Equal variances assumed	14.167	.000	.653	238	.514	.08455593	.12943976	-.17043801	.33954988
	Equal variances not assumed			.653	210.162	.514	.08455593	.12943976	-.17061074	.33972261
Jump occurrence Location (P1)	Equal variances assumed	.019	.890	.212	238	.832	.15937500	.75224432	-1.32253242	1.64128242
	Equal variances not assumed			.212	237.887	.832	.15937500	.75224432	-1.32253602	1.64128602
Jump Length (Lj)	Equal variances assumed	3.214	.074	-.246	238	.806	-.26166667	1.06314105	-2.35603491	1.83270157
	Equal variances not assumed			-.246	223.802	.806	-.26166667	1.06314105	-2.35671416	1.83338083

Prediction accuracy is measured statistically by two tests, the first is mean absolute percentage error (MAPE) and the second is Root mean square error (RMSE). These

two testing methods are usually used to measure how close are the predicted values to that measured in reality (Myttenaere *et.al.*, 2015). Myttenaere show that finding the best model is under the test of mean absolute percentage error (MAPE), the test results are presented in table (3) which shows that the error can be accepted

Table(3) Predicted error test

Measure	MAPE (%)	RMSE with units		R2
1- Discharge (Q)	0.808700	0.009769	l/s	0.998
2- Frg	6.737757	0.234549		0.949
3- d1	0.111823	1.341976	mm	0.887
4- Jump occurrence Location (P1)	14.62861	2.466506	c m	0.858
5- Jump Length (Lj)	16.68013	7.587949	c m	0.833

The highest prediction error (table 3) occurs in the location of starting hydraulic jump (P1) and the Length of jump, this error in measurements may happen due to oscillation pattern of jump and its surface deformation (Wang *et.al.*, 2015). The output of simulation presented in figure (3a) shows reverse flow, forward flow and rollers zone of hydraulic jump. Figure (3b) shows volume fraction of entrained air which appears as Light blue colour. The value of this fraction varied between is 0.18 to 0.28.

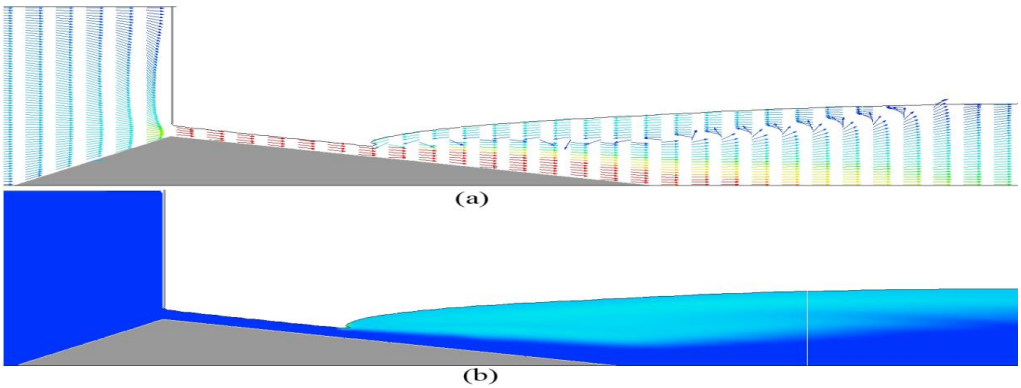

Figure (3) Recirculation region and air mixture percent 0.18 to 0.28 for Froude number Fr1=5.01.

Depending on the definitions in figure (1), where x_1 represent jump toe, d_1 and E_1 are upstream hydraulic jump depth and energy respectively. The variables X, d, and E are any distance, depth and energy along the jump, while u,v and w are the velocity (U) components in the coordinates x,y and respectively. In hydraulic jump, there is a peak rate of energy exchange on each streamwise (x-X1)/d1, the peak value of energy exchange reduces as streamwise value increase. Figure (4) shows the decrease of both relative energy and relative velocity components when streamwise value increase. The kinetic energy exchange process happens first by pressure work flux later this changes into potential energy flux and dissipation, (Mortazavi *et.al.*, 2016). Mortazavi study on horizontal bed shows that the process of exchange takes place in spans of streetwise length of 10 times jump height. The calculated values of streamwise and rate of energy exchange from the simulation output, in this present type of jump B, indicate that the energy exchange average process take place within 6.6, 6.1, 5.8, 5.5 of relative jump height for bed slopes of 0.18, 0.14, 0.10, 0.07 respectively depending on Froude number, jump location. The slope relation to the average values of relative depths at which energy exchange is presented in Figure (5). Figure (6) shows some dimensionless profiles and how these profiles became horizontal before the value of 9.

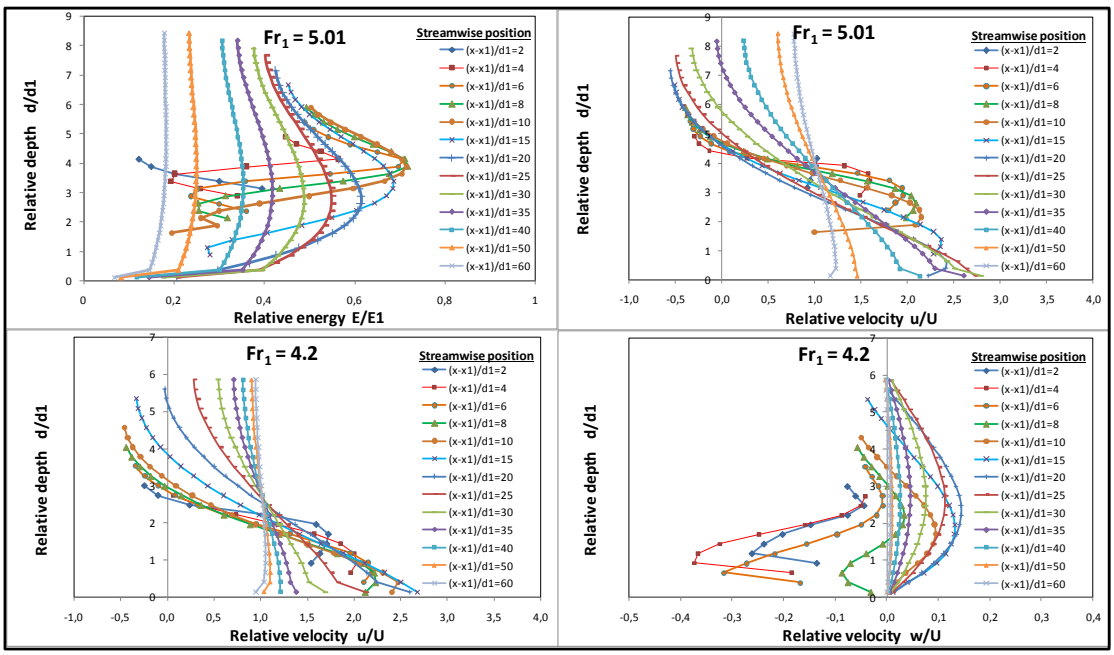

Figure (4) Profiles of relative energy and relative velocities for different streamwise location S= 0.18

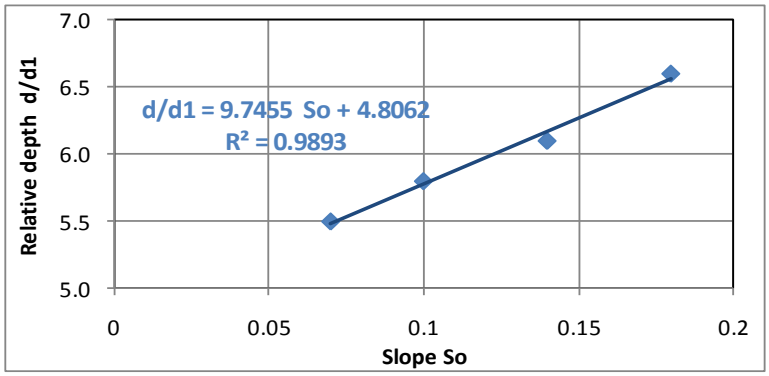

Figure (5) Variation of average relative depth of energy exchange with apron slope

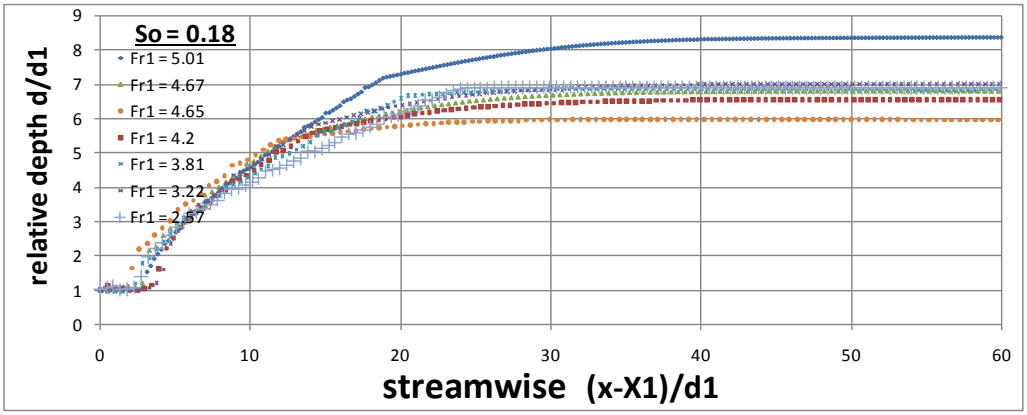

Figure (6) Dimensionless streamwise Profiles for So= 0.18

The simulation data of free surface profile is compared with best correlated power equation of (Wang *and* Chanson, 2013) and with Chansons physical data (Chanson, 2011). The free-surface elevation data showed a similar profile to previous studies as presented in Figure (7). A comparison between figure (4) and (7) leads to

conclude that major part energy lost is happened in the first half length of jump, this cause a rapid increase in flow depth.

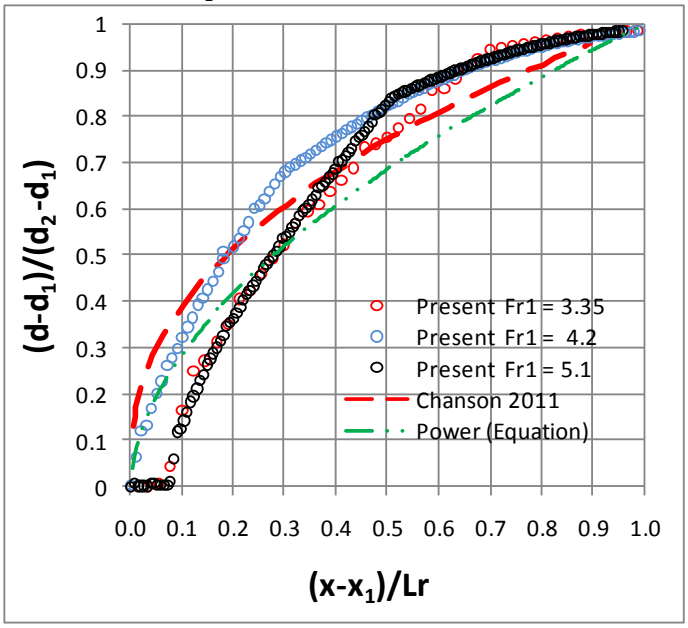

Figure (7) free surface profile comparison with earlier studies.

The simulation outputs are used to calculate dimensionless relative depth (d/d1) and the dimensionless distance (x-X1)/d1. The calculated dimensionless values of free-surface profile have presented in figure (8) for apron slope So=0.18. Figure (8) shows a comparison with results of (Murzyn *and* Chanson, 2009) for different selected values of Froude number. It can be noted that there is a regular increase in jump free surfaces and the then it became horizontal. The shapes and the trend of the relations are nearly the same trend as that in mentioned study for Murzyn and Chanson.

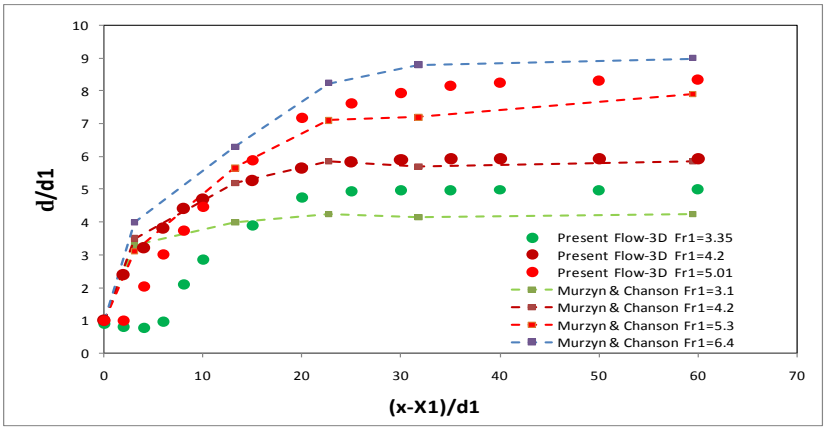

Figure (8) Dimensionless free surface comparison with Murzyn and Chanson (2009).

If d_2^* is denoted as the equivalent depth of jump on horizontal smooth bed, and calculated for the values d_1 and Fr_1 as that on sloping apron, So that calculated value of d_2^* is the second depth as if the total length of hydraulic happens on horizontal bed. A relatvie dimensionless depth can be calculated (Y_{tw}/d_2^*), where Y_{tw} is the measured tail water depth of this investigation. The part of the hydraulic jump which happens on the slope has a length (l) which is measured from the toe of jump to the horizontal bed; this length (l) can be also related to d_2^* as (l/d_2^*). The relation between these two dimensionless parameter have been studied by (Peterka, 1984). Figure (9) shows a

reasonable comparison with experimental study of Peterka for all apron slopes.

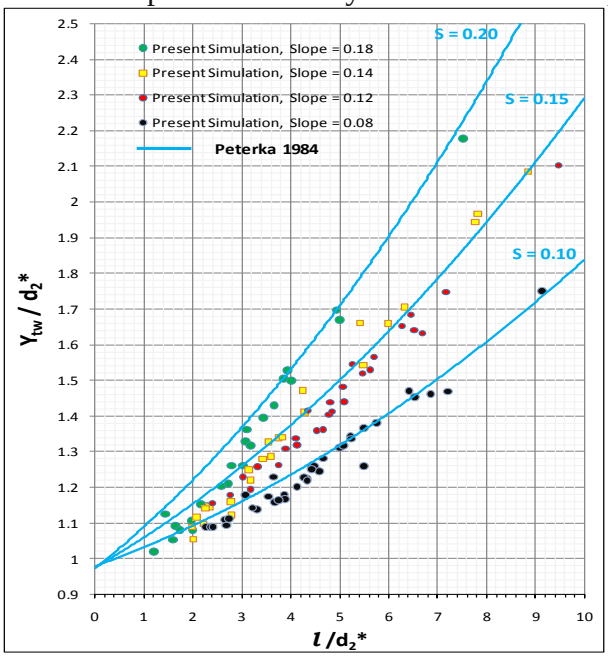

Figure (9). Dimensionless tail water and distance on slopped aprons comparison with Peterka (1984).

Statistical correlation has studied the relation between jump height relative to first jump depth $\left((Y_{tw}-d_1)/d_1\right)$ with other parameters affecting jump characteristics, such as Froude number Fr1, apron slope (So), relative jump length $\left(L_j/dz\right)$ and (d_1/l). The analysis results of IBM-SPSS 20 Package show significant correlation between the variables. The heights Pearson correlation values at 0.01 levels (2-tailed) are (0.945, 0.681, 0.344) for the parameters $\left(Fr_1\,,\ L_j/dz\,,\ d_1/l\right)$ respectively. The Linear regression analysis shows an acceptable mathematical model listed in equation (8).

$$\frac{Y_{tw}-d_1}{d_1} = -0.038 + 0.981Fr_1 - 5.155\,S_o + 0.870\,\frac{d_1}{dz} \dots\dots\dots\dots\dots\dots\dots\dots (8) \qquad R^2 = 0.944$$

Conclusion

The comparison between experimental data and the simulation outputs for a hydraulic jump which happens on sloping apron and ending on horizontal bed leads to the following findings within the study limitations:

1- The volume fraction of blended air after Hydraulic jump toe varied between is 0.18 to 0.28.
2- The energy exchange process take place in within 6.6, 6.1, 5.8, 5.5 of relative jump height for bed slopes of 0.18, 0.14, 0.10, 0.07 respectively depending on Froude number and jump location.

References

Abbaspour A., Farsadizadeh D., Hosseinadeh Dalir A. H., & Sadraddini A. A. ,2009. Numerical study of hydraulic jumps on corrugated beds using turbulence models. *Turkish Journal of Engineering and Environmental Sciences*, *33*(1), 61–72. https://doi.org/10.3906/muh-0901-7

Afzal N., & Bushra A. ,2002. Structure of the turbulent hydraulic jump in a trapezoidal channel. *Journal of Hydraulic Research*, *40*(2), 205–214. https://doi.org/10.1080/00221680209499863

Babaali H., Shamsai A., & Vosoughifar H. ,2014 . Computational Modeling of the Hydraulic Jump in the Stilling Basin with Convergence Walls Using CFD Codes. *Arabian Journal for Science and Engineering*, *40*(2), 381–395. https://doi.org/10.1007/s13369-014-1466-z

Boucher R.F. and Nakayama Y. ,1999 . Introduction to Fluid Mechanics, 759. https://doi.org/10.1111/j.1549-8719.2009.00016.x.Mechanobiology

Carollo F. G., Ferro V., & Pampalone V. , 2007. Hydraulic Jumps on Rough Beds. *Journal of Hydraulic Engineering*, *133*(4) , 440–450. https://doi.org/10.1061/(ASCE)0733-9429(2007)133

Carollo F. G., Ferro V., & Pampalone V. ,2013 . Sequent depth ratio of B-jumps on smooth and rough beds. *Journal of Agricultural Engineering*, *44*(2), 82–86. https://doi.org/10.4081/jae.2013.e12

Chanson H. ,2011 . Hydraulic jumps: turbulence and air bubble entrainment. *Houille Blanche-Revue Internationale De L Eau*, (3), 5–16. https://doi.org/10.1051/lhb/2011026

Chanson H.,2008 . *Jean-Baptiste Charles Joseph Bélanger (1790-1874), The Backwater Equation And The Bélanger Equation*. (S. L. Q. The University of Queensland, Ed.). Brisbane QLD 4072: The University of Queensland, Brisbane QLD 4072, Australia.

Chow V. Te. ,1959 . Open-channel hydraulics. *McGraw-Hill Book Company*, 391–438. https://doi.org/ISBN 07-010776-9

Chow V. Te. ,1967 . *Advances in Hydroscience*. (V. Te Chow, Ed.) (Volume 4). New York: Academic Press. Retrieved from https://books.google.com.sg/books?id=9QLgBAAAQBAJ

Davidson L. ,2017 . Fluid mechanics , turbulent flow and turbulence modeling. *Production*. Chalmers University of Technology, Sweden. Retrieved from http://www.tfd.chalmers.se/~lada/postscript_files/solids-and-fluids_turbulent-flow_turbulence-modelling.pdf

Flow-3D.,2012. *Flow-3D Documentation, Release 10.1.0*. (I. Flow Science, Ed.).

Gumus, V., Simsek, O., Soydan, N. G., Akoz, M. S., & Kirkgoz, M. S.,2016 . Numerical Modeling of Submerged Hydraulic Jump from a Sluice Gate. *Journal of Irrigation and Drainage Engineering*, *142*(1), 4015037. https://doi.org/10.1061/(ASCE)IR.1943-4774.0000948

Henderson F. M.,1966 . *Open Channel Flow*. *Macmilan Pubishing co., Inc.* New York: Macmilan Pubishing co., Inc.

Hughes W. C., & Flack J. E. ,1984. Hydraulic jump properties over a rough bed. *Journal of Hydraulic Engineering - ASCE*. https://doi.org/10.1061/(ASCE)0733-9429(1984)110:12(1755)

Husain D., Alhamid A. A., & Negm A. M. ,1994 . Length and depth of hydraulic jump in sloping channels. *Journal of Hydraulic Research*, *32*(6), 899–910. https://doi.org/10.1080/00221689409498697

Imran H. M., & Akib S. ,2013 . A review of hydraulic jump properties in different channel bed conditions. *Life Science Journal*, *10*(2), 126–130.

Karbasi M. ,2016. Estimation of classical hydraulic jump length using teaching – learning based optimization algorithm. *Journal of Materials and Environmental Science*, *7*(8), 2947–2954.

Kim Y., Choi G., Park H., & Byeon S. ,2015 . Hydraulic jump and energy dissipation with sluice gate. *Water (Switzerland)*, *7*(9), 5115–5133. https://doi.org/10.3390/w7095115

Mortazavi M., Le Chenadec V., Moin P., & Mani A.,2016 . Direct numerical simulation of a turbulent hydraulic jump: turbulence statistics and

air entrainment. *Journal of Fluid Mechanics*, *797*(November), 60–94. https://doi.org/10.1017/jfm.2016.230

Mouangue R., Beda T., & Murzyn F.,2013 . Characterization of Hydraulic Jump over an Obstacle in an Open-Channel Flow, *2*(5), 71–84. https://doi.org/10.5923/j.ijhe.20130205.01

Murzyn F., & Chanson H. ,2008 . Experimental assessment of scale effects affecting two-phase flow properties in hydraulic jumps. *Experiments in Fluids*, *45*(3), 513–521. https://doi.org/10.1007/s00348-008-0494-4

Murzyn F., & Chanson H. ,2009. Non intrusive measurement technique for dynamic free-surface characteristics in hydraulic jumps. In *33rd IAHR Congress: Water Engineering for a Sustainable Environment, Congress 9-14 August 2009* (pp. 3511–3518). International Association of Hydraulic Engineering & Resear ch (IAHR). https://doi.org/10.1017/CBO9781107415324.004

Myttenaere A. De, Golden B., Myttenaere A. De & Golden B.,2015 . Using the Mean Absolute Percentage Error for Regression Models To cite this version : In *ESANN 2015 proceedings, European Symposium on Artificial Neural Networks, Computational Intelligence and Machine Learning. Bruges (Belgium), 22-24 April 2015, i6doc.com pub* (pp. 22–24).

Negm A. M., Abdel-Aal G. M., & Habib A. A.,2003 . Effect of location of negative step on hydraulic characteristics of jumps in radial ... In *Proc. of 7th Alazhar Engineering Int. Conf. (AEIC'2003), April 7-10, Faculty of Engineering, Alazhar University, Naser City, Cairo, Egypt, 2003.*

Peterka A. J. ,1984 . Hydraulic design of stilling basins and energy dissipators. *Water Resources Technical Publication*, (25), 240.

Rostami, F., Shahrokhi, M., Md Saod, M. A., & Sabbagh Yazdi, S. R. (2013). 'Numerical simulation of undular hydraulic jump on smooth bed using volume of fluid method. *Applied Mathematical Modelling*, *37*(1514–1522), 2302. https://doi.org/10.1016/j.apm.2014.01.010

Saeed-Reza S., Fatemeh R., & Mastorakis N. ,2007 . Turbulent Modeling Effects on Finite Volume Solution of Three Dimensional Aerated Hydraulic Jumps using Volume of Fluid. In *12th WSEAS Int. Conf. on Applied Mathematics, Cairo, Egypt, December 29-31, 2007* (pp. 168–174).

Schulz H. ., Simões A. L. ., & Nóbrega J. ,2015 . Roller lengths , sequent depths , surface profiles for pre-design of dissipation basins. In *2nd International Workshop on Hydraulic Structures: Data Validation Coimbra, Portugal, 7-9 May 2015*. https://doi.org/10.13140/RG.2.1.3027.0889

Sitong W., & Rajaratnam N.,1996 . Transition from hydraulic jump to open channel flow. *Journal of Hydraulic Engineering*.

Subramanya K.,2009. *Flow in Open Channels* (Third Edit).New Delhi: Tata McGraw-Hill. Retrieved from https://books.google.es/books/about/Flow_in_Open_Channels.html?id=haljh3BO_1IC&pgis=1

Velioglu D., Tokyay N. D., & Dincer A.,2015 . A Numerical and Experimental Study on the Characteristics of Hydraulic Jumps on Rough Beds. In *E-proceedings of the 36th IAHR World Congress 28 June – 3 July, 2015, The Hague, the Netherlands*. IAHR.

Versteeg H. K., & Malalasekera W. ,2007. *An Introduction to Computational Fluid Dynamics* (Second Edi). Edinburgh Gate: Pearson Education Limited England.

Wang H., & Chanson H.,2013 . Air entrainment and turbulent fluctuations in hydraulic jumps. *Urban Water Journal*. Taylor & Francis. https://doi.org/10.1080/1573062X.2013.847464

Wang H., Murzyn F., & Chanson H.,2015 . Interaction between free-surface, two-phase flow and total pressure in hydraulic jump. *Experimental Thermal and Fluid Science*, *64*(February), 30–41. https://doi.org/10.1016/j.expthermflusci.2015.02.003

Witt A. M. ,2014 . *Analytical and Numerical Investigation of An Air Entraining Hydraulic Jump*. Faculty of University of Minnesota.

Yakhot V., & Orszag S. A. ,1986 . Renormalization Group Analysis of Turbulence. *Journal of Scientific Computing*, *1*(1), 1–51.

Yakhot, V., & Smith, L. M. (1992). The renormalization group, the ε -expansion and derivation of turbulence models. *Journal of Scientific Computing*, *7*(1), 35–61.

Yakhot, V., Thangam, S., Gatski, T., Orszg, S., & Speziale, C. (1991). Development of Turbulence Models for Shear Flows by a Double Expansion technique. *NASA, Institute for Computer Application in Science and Engineering*, (July). https://doi.org/10.1063/1.858424

Zhang G., Wang H., & Chanson H. ,2013 . Turbulence and aeration in hydraulic jumps: Free-surface fluctuation and integral turbulent scale measurements. *Environmental Fluid Mechanics*, *13*(2), 189–204. https://doi.org/10.1007/s10652-012-9254-3